

## This file includes:

Materials and Methods  
SupplementaryText  
Tables S1 to S2

## Materials and Methods

*Experimental Approach:* Layers of  $500 \pm 50$  nm of amorphous  $\text{NH}_3$  (Matheson; 99.999 %) and D3-ammonia (Isotopes Inc; 99+ % D) were deposited in separate experiments on a silver substrate interfaced to a cold finger at a temperature of  $5.5 \pm 0.2$  K in a vacuum chamber with a base pressure of a few  $10^{-11}$  torr via gas phase deposition using a glass capillary array<sup>[1]</sup>. The deposition time was 3 min at a pressure of  $(4 \pm 2) \times 10^{-8}$  torr. The ice thicknesses were determined using in situ helium-neon (He-Ne) laser interferometry<sup>[2]</sup> with a laser wavelength  $\lambda$  of 632.8 nm and a refractive index  $n$  of the ammonia ice at 5.5 K of  $1.35 \pm 0.05$ <sup>[3]</sup> via equation (1), where  $d$  is the ice thickness and  $\theta$  is the angle of incidence of the laser with respect to the surface normal ( $4^\circ$ ).

$$(1) \quad d = \frac{N_f \lambda}{2\sqrt{n^2 - \sin^2 \theta}}$$

Each sample was then irradiated for 60 min with 5 keV electrons at a current of  $15 \pm 2$  nA by scanning the electron beam over the target surface of  $1.0 \pm 0.1$  cm<sup>2</sup> at an angle of  $70^\circ$  with respect to the surface normal of the substrate. The average deposited dose  $D$  per ammonia molecule can be calculated using equation (2), where  $I$ ,  $t$ ,  $m$ ,  $e$ ,  $N_A$ ,  $\rho$  and  $A$  and  $E_{\text{init}}$  are the irradiation current, irradiation time, molecular mass of the molecule, the electron charge, Avogadro's constant, the density of the ice, the irradiated area of the ice, and the initial kinetic energy of the electrons, respectively.

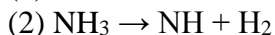
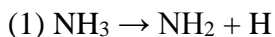
$$(2) \quad D = \frac{I t m}{e N_A \rho A l} (E_{\text{init}} - f_{\text{trans}} E_{\text{trans}} - f_{\text{bs}} E_{\text{bs}}),$$

The values  $f_{\text{trans}}$ ,  $f_{\text{bs}}$ ,  $E_{\text{bs}}$ ,  $E_{\text{trans}}$  and  $l$  denote the fraction of electrons transmitted through the ice, the fraction of electrons which are backscattered, the average kinetic energy of the backscattered electrons, the average kinetic energy of the transmitted electrons, and the average penetration depth of the electrons. These values are determined exploiting the Monte-Carlo simulation program CASINO<sup>[4]</sup> averaging over 20,000 trajectories. The deposited energy per ammonia molecule in this experiments is determined to be  $1.9 \pm 0.2$  eV with the simulation parameters summarized in Table S1. After the irradiation, the ice was kept at 5.5 K for one hour. During the irradiation and the equilibration phase, infrared spectra (FTIR, Nicolet6700) were recorded from 6000 to 500 cm<sup>-1</sup> with a resolution of 4 cm<sup>-1</sup>. The substrate was then warmed up with a constant rate of 0.5 Kmin<sup>-1</sup> to 300 K. Molecules subliming into the gas phase were photo ionized at 10.49 eV and detected using a reflectron time-of-flight mass spectrometer (ReTOF)<sup>[1]</sup>. Vacuum ultraviolet (VUV) light at 10.49 eV was produced by non-resonant four wave mixing of

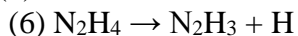
the third harmonic of a Nd:YAG laser at 30 Hz resulting in a pulse width of  $10 \pm 4$  ns and  $(4 \pm 2) \times 10^{12}$  photons  $\text{cm}^{-2} \text{s}^{-1}$ . The VUV beam had a diameter of  $1.0 \pm 0.1$  mm and was directed over the substrate parallel to its surface at a distance of  $2.0 \pm 0.1$  mm. Molecules which were ionized above the substrate were accelerated into the ReTOF and detected using microchannel plates.

The infrared spectra are in line with an earlier study<sup>[5]</sup> and show mainly a decrease in the ammonia bands and an emerging signal of the hydrazine molecule ( $\text{N}_2\text{H}_4$ ) at 900, 1151 and  $3185 \text{ cm}^{-1}$ . This earlier study also exploited a residual gas analyzer (quadrupole mass spectrometer; QMS) with electron impact (EI) ionization (100 eV). The dominant products subliming into the gas phase were identified to be molecular hydrogen ( $\text{H}_2$ ), molecular nitrogen ( $\text{N}_2$ ), at least one isomer of diimide/trans diazene ( $\text{N}_2\text{H}_2$ ), and hydrazine ( $\text{N}_2\text{H}_4$ ). A comparison between the earlier QMS-EI<sup>[6]</sup> setup and the present Re-TOF-PI<sup>[7]</sup> study suggests that the Re-TOF coupled with VUV photo ionization at 10.49 eV not only significantly reduces the background counts, but also increases the signal-to-noise of the experiments essentially improving the sensitivity of the detection scheme by a factor of at least 30. The triazane molecule ( $\text{N}_3\text{H}_5$ ) as detected via Re-TOF is formed at levels of about 10 % of hydrazine ( $\text{N}_2\text{H}_4$ ). At these levels, triazane could not have been observed in the earlier experiment exploiting QMS-EI, where hydrazine ( $\text{N}_2\text{H}_4$ ) was barely above the detection threshold of the system. Similarly, accounting for the computed infrared absorption coefficient of the most intense fundamental of triazane at  $1007 \text{ cm}^{-1}$  suggests that triazane is below the detection levels via infrared spectroscopy.

We would like to comment briefly on potential reaction pathways to form triazane ( $\text{N}_3\text{H}_5$ ). Due to the lack of intensity in the infrared spectrum, no temporal profiles and hence no kinetic information on synthetic pathways to triazane can be obtained. Therefore, the following considerations shall be taken as *feasible* reaction pathways. Upon interaction of ionizing radiation with the energetic electrons, ammonia was found to fragment via a predominant atomic hydrogen channel and to a lesser extent via molecular hydrogen loss (reactions (1) - (2))<sup>[8]</sup>



Hydrazine ( $\text{N}_2\text{H}_4$ ), which in turn is formed via radical-radical recombination of two amidogen radicals ( $\text{NH}_2$ ) (reaction (3)) or via insertion of nitrene ( $\text{NH}$ ) into the nitrogen – hydrogen bond of ammonia ( $\text{NH}_3$ )<sup>[5]</sup>, can react with nitrene ( $\text{NH}$ ) yielding triazane ( $\text{N}_3\text{H}_5$ ) (reaction (5)). Alternatively, hydrazine ( $\text{N}_2\text{H}_4$ ) can be radiolyzed to the hydrazinyl radical ( $\text{N}_2\text{H}_3$ ), which in turn undergoes radical-radical recombination with the amidogen radical ( $\text{NH}_2$ ) (reactions ((6) and (7)) yielding triazane.



*Theoretical Methods:* The triazane decomposition channels are investigated by *ab initio* electronic structure calculations. The optimized geometries and harmonic frequencies of reactant (and its cation), intermediate, transition states, and products are predicted by the hybrid density functional B3LYP<sup>[9]</sup> level of theory with the cc-pVTZ basis set. The energies of these species were refined employing the CCSD(T)/cc-pVTZ with B3LYP/cc-pVTZ zero-point energy corrections.<sup>[10]</sup> The GAUSSIAN09 program<sup>[11]</sup> was utilized in the electronic structure calculations. The energy computation is expected to have accuracy of 10 kJ mol<sup>-1</sup>. The adiabatic ionization energy was then calculated by taking the energy difference between the ionic and the lowest lying neutral state (I) calculated by CCSD(T)/cc-pVTZ with B3LYP/cc-pVTZ zero-point energy correction. Previous computations at this level compared with experimentally derived ionization energies suggests that the ionization energies derived from the CCSD(T)/cc-pVTZ with B3LYP/cc-pVTZ zero-point energy correction method are accurate within  $\pm 0.2$  eV<sup>[12]</sup>.

**Table S1.** Data applied to calculate the irradiation dose per molecule. \* marks values from CASINO simulations.

initial kinetic energy of the electrons, $E_{\text{init}}$	5 keV
irradiation current, I	$15 \pm 2$ nA
total number of electrons	$(3.4 \pm 0.3) \times 10^{14}$
average kinetic energy of backscattered electrons, $E_{\text{bs}}^*$	$3.2 \pm 0.9$ keV
fraction of backscattered electrons, $f_{\text{bs}}^*$	$0.3 \pm 0.1$
average kinetic energy of transmitted electrons, $E_{\text{trans}}^*$ ,	$1.0 \pm 0.5$ keV
fraction of transmitted electrons, $f_{\text{trans}}^*$	$0.16 \pm 0.05$
average penetration depth, $l^*$	$350 \pm 80$ nm
density of the ice, $\rho$	$0.66 \pm 0.05$ g cm <sup>-3</sup>
irradiated area, A	$1.0 \pm 0.1$ cm <sup>2</sup>
total number of molecules processed	$(8 \pm 2) \times 10^{17}$
dose per molecule, D	$1.9 \pm 0.2$ eV

**Table S2.** Energies of the reactants, intermediates, products, and transition states.

	B3LYP/ cc-pVTZ <sup>a</sup>	E <sub>zpc</sub> <sup>b</sup>	CCSD(T)/ cc-pVTZ	IP(eV) <sup>c</sup>	IP(eV) <sup>d</sup>
NH <sub>2</sub> NHNH <sub>2</sub> ( <sup>1</sup> A)	-167.192258	0.070471	-166.940565	0.00	0.00
NH <sub>2</sub> NHNH <sub>2</sub> <sup>+</sup> ( <sup>2</sup> A')	-166.915139	0.069796	-166.656608	7.54	7.71
	B3LYP/ cc-pVTZ <sup>a</sup>	E <sub>zpc</sub> <sup>b</sup>	CCSD(T)/ cc-pVTZ	E(kJ/mol) <sup>e</sup>	E(kJ/mol) <sup>f</sup>
NH <sub>2</sub> NHNH <sub>2</sub> (X <sup>1</sup> A')	-167.192258	0.070471	-166.940565	0	0
NH <sub>2</sub> NHNH <sub>2</sub> <sup>+</sup> (X <sup>2</sup> A')	-166.915139	0.069796	-166.656608	728	744
NH <sub>2</sub> NHNH <sub>2</sub> '(X <sup>1</sup> A)	-167.190756	0.070288	-166.938882	4	4
NH <sub>2</sub> NHNH <sub>2</sub> "(X <sup>1</sup> A)	-167.184014	0.069754	-166.931014	22	23
INT(X <sup>1</sup> A)	-167.132931	0.069478	-166.877622	152	159
N <sub>2</sub> H <sub>4</sub> (X <sup>1</sup> A)	-111.862641	0.053219	-111.698545		
NH <sub>3</sub> (X <sup>1</sup> A <sub>1</sub> )	-56.550474	0.034252	-56.473157		
trans HNNH(X <sup>1</sup> A <sub>g</sub> )	-110.657077	0.028316	-110.477660		
cis HNNH(X <sup>1</sup> A <sub>1</sub> )	-110.649782	0.027625	-110.469421		
H <sub>2</sub> NN(X <sup>1</sup> A <sub>1</sub> )	-110.624527	0.026519	-110.436759		
TS3	-167.103201	0.062952	-166.844662	234	232
TS4	-167.129837	0.062446	-166.863852	164	180
TS1	-167.093493	0.064313	-166.834452	259	258
TS2	-167.123036	0.064377	-166.861913	182	191
<sup>1</sup> NH + N <sub>2</sub> H <sub>4</sub>	-167.016683	0.060720	-166.768164	461	428
<sup>3</sup> NH + N <sub>2</sub> H <sub>4</sub>	-167.098047	0.060623	-166.839231	247	240
NH <sub>2</sub> + NHNH <sub>2</sub>	-167.122421	0.058366	-166.851544	183	202
NH <sub>3</sub> + trans HNNH	-167.207551	0.062568	-166.950817	-40	-48
NH <sub>3</sub> + cis HNNH	-167.200256	0.061877	-166.942578	-21	-28
NH <sub>3</sub> + NNH <sub>2</sub>	-167.175001	0.060771	-166.909916	45	55

<sup>a</sup> B3LYP/cc-pVTZ energy with zero-point energy correction in hartree.<sup>b</sup> zero-point energy by B3LYP/cc-pVTZ in hartree.<sup>c</sup> ionization potential by B3LYP/cc-pVTZ with zero-point energy correction.<sup>d</sup> ionization potential by CCSD(T)/cc-pVTZ with B3LYP/cc-pVTZ zero-point energy correction.<sup>e</sup> relative energy by B3LYP/cc-pVTZ with zero-point energy correction.<sup>f</sup> relative energy by CCSD(T)/cc-pVTZ with B3LYP/cc-pVTZ zero-point energy correction.

- [1] B. M. Jones, R. I. Kaiser, *JPhChL* **2013**, *4*, 1965-1971.
- [2] a) O. S. Heavens, *Optical Properties of Thin Solid Films*, Butterworths Scientific Publications, London, **1955**; b) M. S. Westley, G. A. Baratta, R. A. Baragiola, *JChPh* **1998**, *108*, 3321-3326.
- [3] M. Á. Satorre, J. Leliwa-Kopystynski, C. Santonja, R. Luna, *Icar* **2013**, *225*, 703-708.
- [4] D. Drouin, A. R. Couture, D. Joly, X. Tastet, V. Aimez, R. Gauvin, *Scanning* **2007**, *29*, 92-101.
- [5] W. Zheng, D. Jewitt, Y. Osamura, R. I. Kaiser, *ApJ* **2008**, *674*, 1242-1250.
- [6] C. J. Bennett, C. S. Jamieson, Y. Osamura, R. I. Kaiser, *ApJ* **2005**, *624*, 1097-1115.
- [7] R. I. Kaiser, S. Maity, B. M. Jones, *PCCP* **2014**, *16*, 3399-3424.
- [8] C. J. Bennett, B. Jones, J. E. Knox, J. Perry, Y. S. Kim, R. I. Kaiser, *ApJ* **2010**, *723*, 641-648.
- [9] a) A. D. Becke, *JChPh* **1993**, *98*, 5648-5652; b) A. D. Becke, *JChPh* **1992**, *96*, 2155-2160; c) A. D. Becke, *JChPh* **1992**, *97*, 9173-9177; d) C. Lee, W. Yang, R. G. Parr, *Physical Review B* **1988**, *37*, 785-789.
- [10] a) G. D. Purvis, R. J. Bartlett, *JChPh* **1982**, *76*, 1910-1918; b) C. Hampel, K. A. Peterson, H.-J. Werner, *Chemical Physics Letters* **1992**, *190*, 1-12; c) P. J. Knowles, C. Hampel, H. J. Werner, *JChPh* **1993**, *99*, 5219-5227; d) M. J. O. Deegan, P. J. Knowles, *Chemical Physics Letters* **1994**, *227*, 321-326.
- [11] M. J. Frisch, G. W. Trucks, H. B. Schlegel, G. E. Scuseria, M. A. Robb, J. R. Cheeseman, G. Scalmani, V. Barone, B. Mennucci, G. A. Petersson, H. Nakatsuji, M. Caricato, X. Li, H. P. Hratchian, A. F. Izmaylov, J. Bloino, G. Zheng, J. L. Sonnenberg, M. Hada, M. Ehara, K. Toyota, R. Fukuda, J. Hasegawa, M. Ishida, T. Nakajima, Y. Honda, O. Kitao, H. Nakai, T. Vreven, J. A. Montgomery Jr., J. E. Peralta, F. Ogliaro, M. J. Bearpark, J. Heyd, E. N. Brothers, K. N. Kudin, V. N. Staroverov, R. Kobayashi, J. Normand, K. Raghavachari, A. P. Rendell, J. C. Burant, S. S. Iyengar, J. Tomasi, M. Cossi, N. Rega, N. J. Millam, M. Klene, J. E. Knox, J. B. Cross, V. Bakken, C. Adamo, J. Jaramillo, R. Gomperts, R. E. Stratmann, O. Yazyev, A. J. Austin, R. Cammi, C. Pomelli, J. W. Ochterski, R. L. Martin, K. Morokuma, V. G. Zakrzewski, G. A. Voth, P. Salvador, J. J. Dannenberg, S. Dapprich, A. D. Daniels, Ö. Farkas, J. B. Foresman, J. V. Ortiz, J. Cioslowski, D. J. Fox, Gaussian, Inc., Wallingford, CT, USA, **2009**.
- [12] a) O. Kostko, J. Zhou, B. J. Sun, J. S. Lie, A. H. Chang, R. I. Kaiser, M. Ahmed, *ApJ* **2010**, *717*, 674; b) I. K. Ralf, P. K. Sergey, M. M. Alexander, K. Oleg. A. Musahid, *ApJ* **2012**, *761*, 178.